

Fig. 4.14 SEM pictures of the surface morphology treated by hydrogen plasma for (a) 5 min, (b) 15min, (c) 30 min and (d) 45 min.

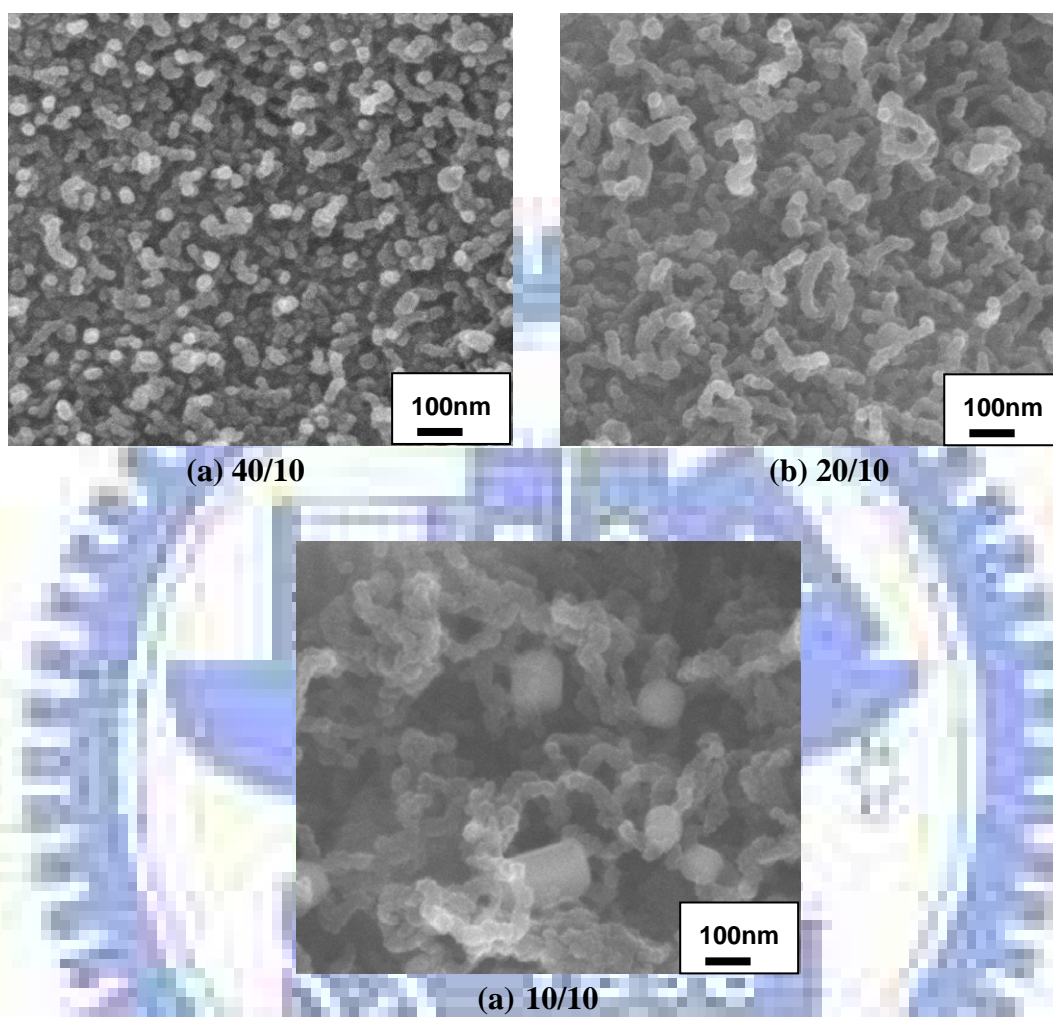


Fig. 4.15 SEM images of different Methane Concentration under the growth condition at 200 W and 6 Torr for 30 min, (a) $\text{H}_2/\text{CH}_4=40/10$ sccm, (b) $\text{H}_2/\text{CH}_4=20/10$ sccm, (c) $\text{H}_2/\text{CH}_4=10/10$ sccm.

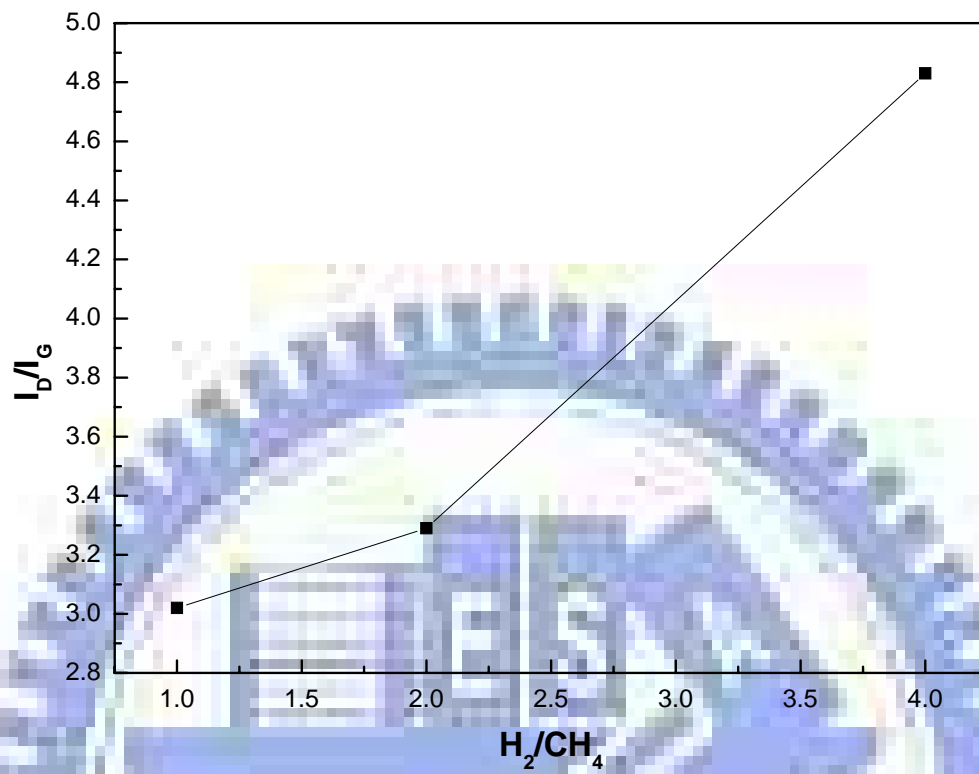


Fig. 4.16 I_D/I_G ratio varies with H_2/CH_4 ratio of 150 W and 6 Torr for 30 min.

4.2.3 Effect of Growth Time of Carbon Nanotubes

Fig. 4.17 showed the SEM pictures of the CNTs grown on 150 W (555 °C) for different growth time with H₂-CH₄ gases. The growth time were 15 min, 30 min, 45 min, 60 min, respectively. Randomly oriented CNTs have grown on glass structure at any growth time. The diameter and length of CNTs increased with increasing the growth time. The diameter of CNTs was from the range of about 20 nm for 15 min to about 70 nm for 60 min. The tubes showed curved structures. Most of the tubes had a bright dot at the tip, indicating electron reflection from metal particles. Two growth modes, tip growth and base growth, have been identified for the catalytic growth mechanism of carbon filaments. In this respect, the growth of CNTs was found to be the tip growth type.

In fig. 4.18, it showed the SEM images of different growth time of the CNTs on 200 W at 6 Torr. Unlike the samples of solution deposition method, the samples were not bend or damaging under 200 W (about 620 °C) for any growth time. The reason was catalyst metal particles prepared by sol-gel method, which were covered with surfactant, might be more stable at higher temperature, allowing high temperature MWNT growth [60]. As the growth time increased, the CNT became larger from the range of about 20 nm for 15 min to about 80 nm for 60 min.

Table 4.4 showed the I_D/I_G ratio of Raman spectrum under 150 W and 200 W, respectively. The I_D/I_G ratio decreased as increasing the growth time on 150 W. This result also showed on 200 W. The I_D/I_G ratio curve slants toward down, indicating a better graphitization as growth increasing.

4.2.4 Effect of MPCVD Power

Compared fig. 4.17 and fig. 4.18, as MPCVD power increased, the diameter and length of CNTs obviously increase from the SEM observation. In table 4.4 and in fig.

4.19, the I_D/I_G ratio decreased as power increased from 150 W to 200 W under the same growth time. It implied that the defective structure containing amorphous carbonaceous particles was effectively removed by plasma during growth at higher temperature.

4.2.5 TEM Analysis of Carbon Nanotubes

Fig. 4.20 showed the TEM images of CNTs grown on the thick film prepared by sol-gel method under 200 W for 60 min. There were two kinds of CNTs grown on the samples. One was herringbone-like structure in fig. 4.20 (a), and the other one is like carbon nanotube showed in fig. 4.20 (b). The diameter of the two structures were almost the same about 50 nm. Both two tubes showed curved structures, and the edge and interior of the CNTs showed many defects. It was likely that pentagons and heptagons formed defective edges which eventually induced bending in carbon nanotubes.

Fig. 4.21 showed HRTEM images of carbon nanotubes of herringbone-like structure in fig. 4.20 (a). Fig. 4.24 (a) represented the catalyst metal particle located at the tips of tubes. The metal particle about 40 nm was embedded in the graphitic layer. From the body image of the tube in fig. 4.21 (b), detailed TEM analysis indicated that the CNT has a herringbone-like structure with hollow compartment. Fig. 4.22 showed the EDX spectrum of the metal tip of the fig. 4.21 (b). The metal particle was composed of Ni.

4.2.6 Field Emission Characteristics

Fig. 4.23 showed the I-V characteristics. The samples were grown at 150 W for 30 min and 200 W for 60 min, respectively. A turn-on field, E_{to} , is defined as the field to give an emission current density of $10 \mu\text{A}/\text{cm}^2$. The turn-on fields were $5.4 \mu\text{A}/\text{cm}^2$

for 200 W sample and $6.4 \mu\text{A}/\text{cm}^2$ for 150 W sample. It shows that under higher power the length of CNTs is higher, and the current density become smaller leading to better field emission properties. However the turn-on field value is larger than the solution deposition method ($3.2 \mu\text{A}/\text{cm}^2$). The reason is that the length of CNTs grown on the thick film prepared by solution deposition method is longer than sol-gel method. And the surface roughness of thick films prepared by solution deposition method is also larger. These properties contribute to the better field emission stability of the sample prepared by solution deposition method.

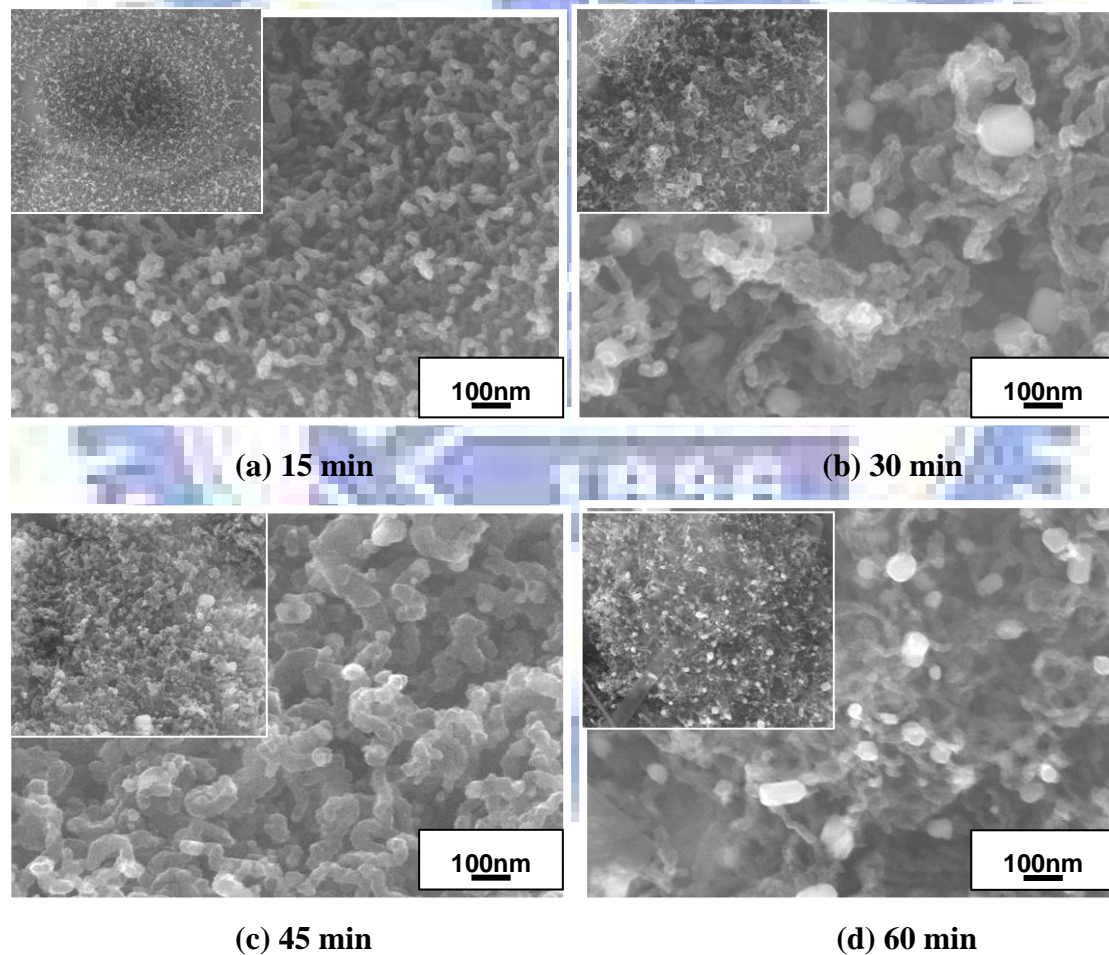


Fig. 4.17 SEM images of surface under the growth condition of $\text{H}_2/\text{CH}_4=10/10$ at the power of 150 W and the pressure of 6 Torr: (a) for 15 min, (b) for 30 min, (c) for 45 min, and (d) for 60 min. The inset diagram is the minification.

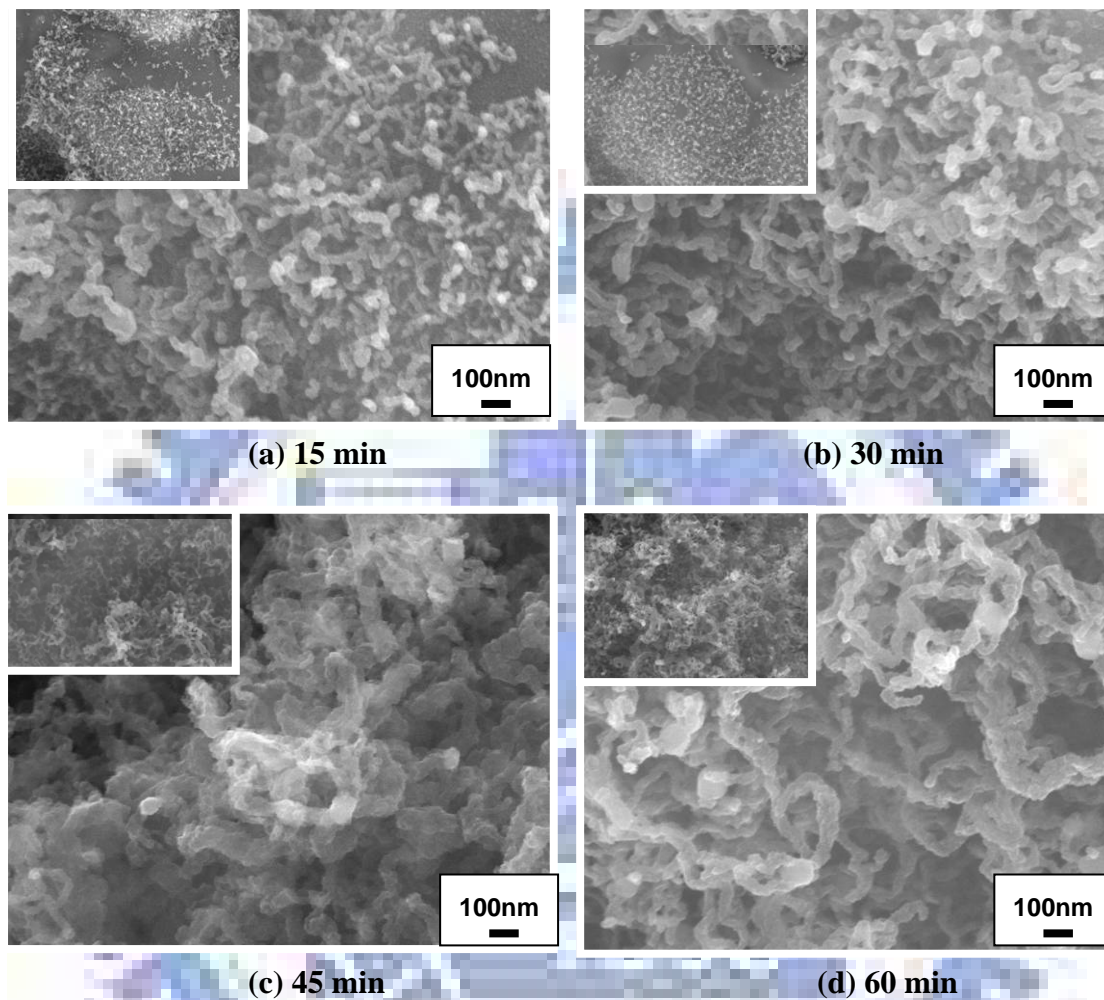


Fig 4.18 SEM images of surface under the growth condition of $H_2/CH_4=10/10$ at the power of 200 W and the pressure of 6 Torr: (a) for 15 min, (b) for 30 min, (c) for 45 min, and (d) for 60 min. The inset diagram is the minification.

150W	15min	30min	45min	60min
D band	145342	238500	322053	762621
G band	50476	78998	159600	268073
I_D/I_G	3.062	3.020	3.018	2.845
condition	No bending	No bending	No bending	No bending

(a)

200W	15min	30min	45min	60min
D band	430629	196748	716301	631987
G band	150595	69360	261837	251658
I_D/I_G	2.860	2.837	2.736	2.511
condition	No bending	No bending	No bending	No bending

(b)

Table 4.4 Data of Raman spectra for different growth time, (a) the MPCVD power of 150 W, (b) 200 W.

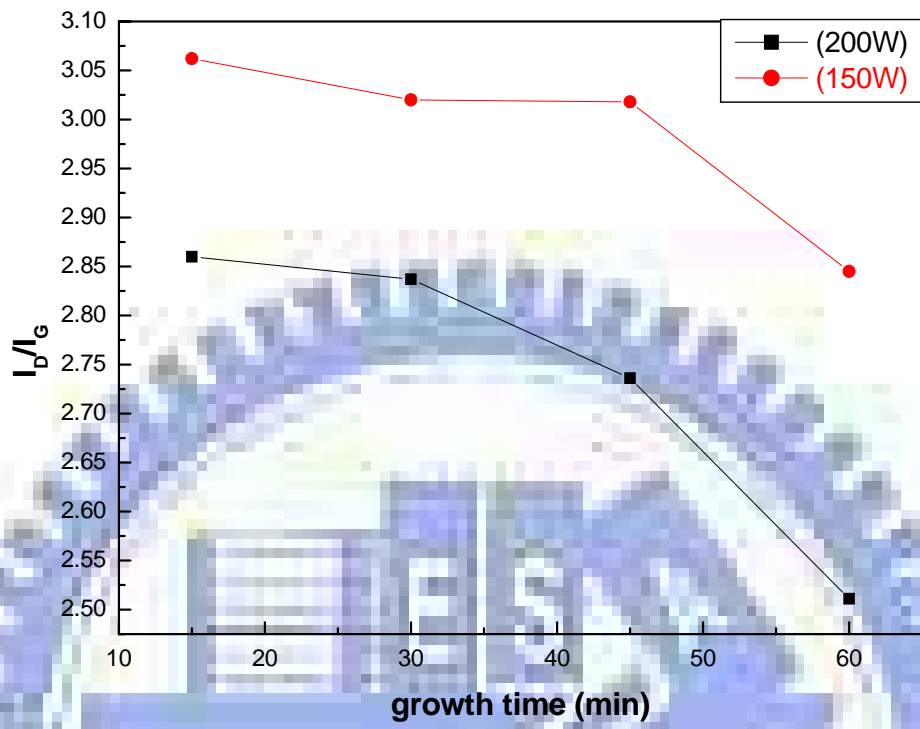
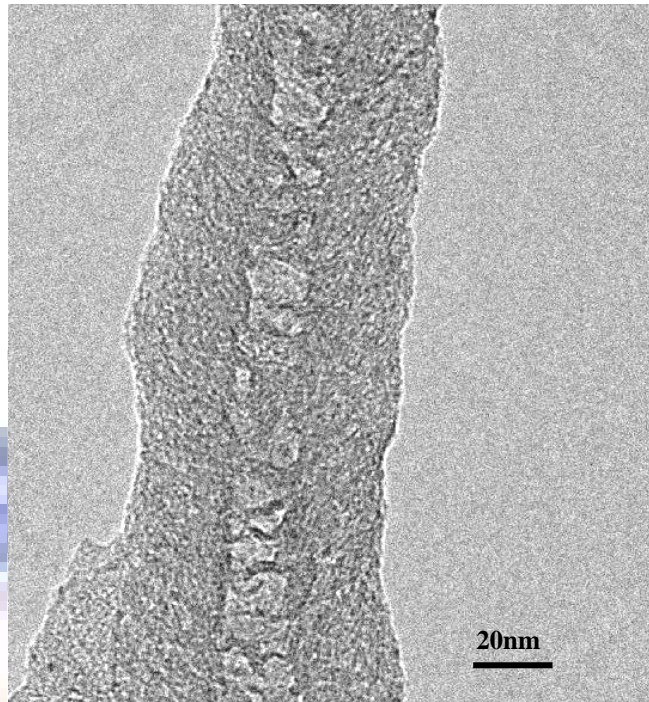
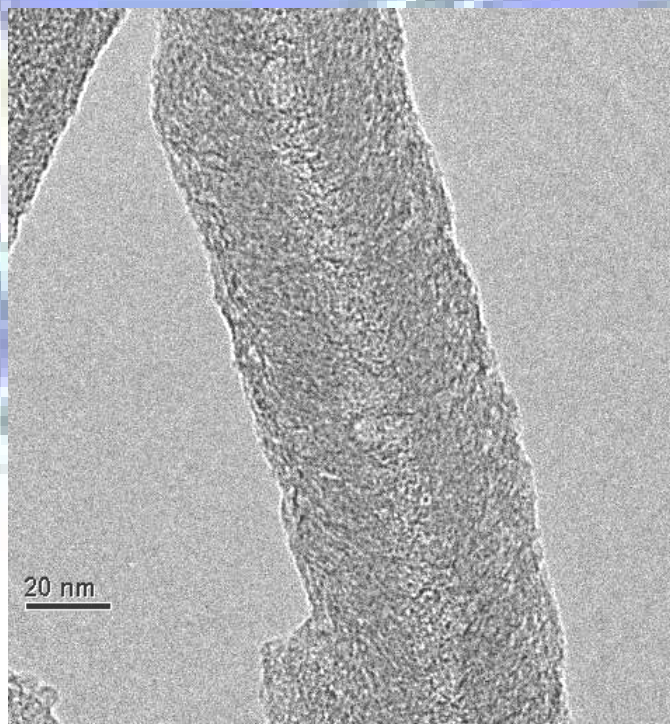


Fig. 4.19 I_D/I_G ratio varied with different growth time of $H_2/CH_4=10/10$ under 150 W and 200 W.

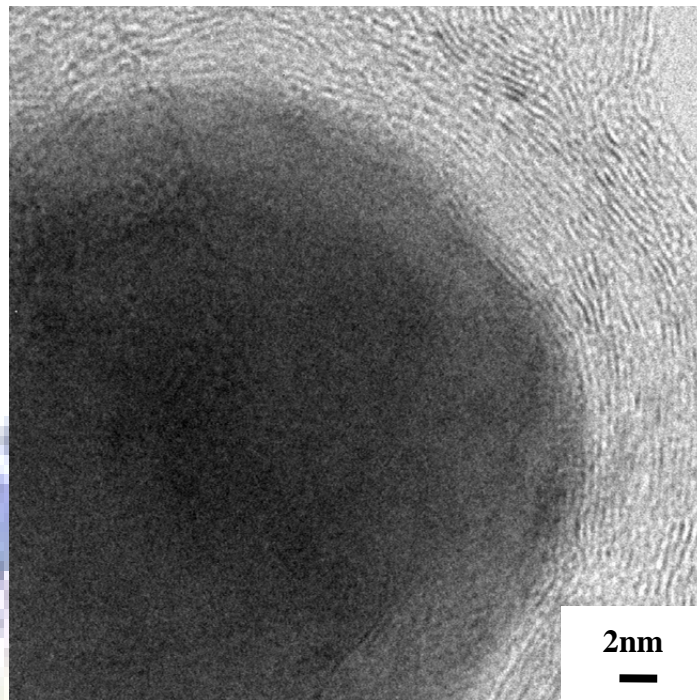


(a)

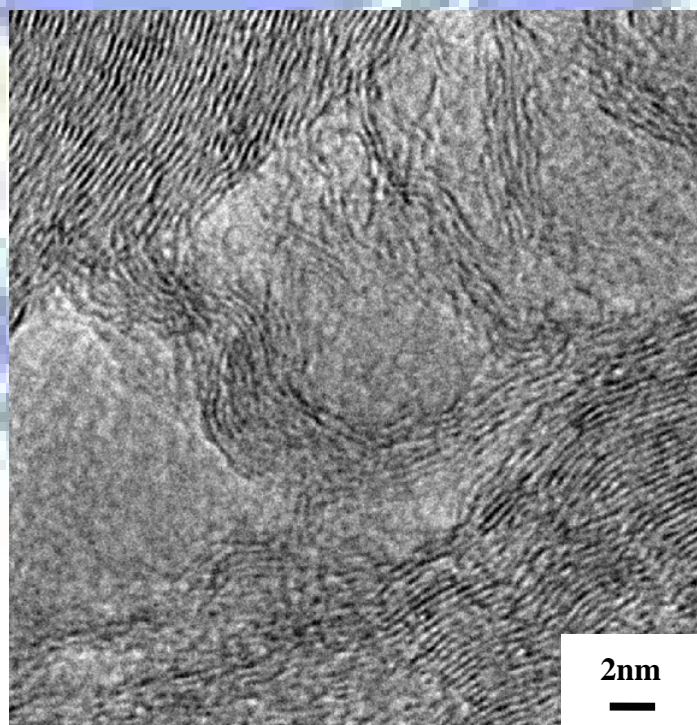


(b)

Fig. 4.20 TEM images of carbon nanotubes. (a) herringbone-like structure, (b) carbon nanontube structure.



(a) at the tip



(a) at the body

Fig. 4.21 HRTEM images of carbon nanotubes, (a) at the tip, (b) at the body.

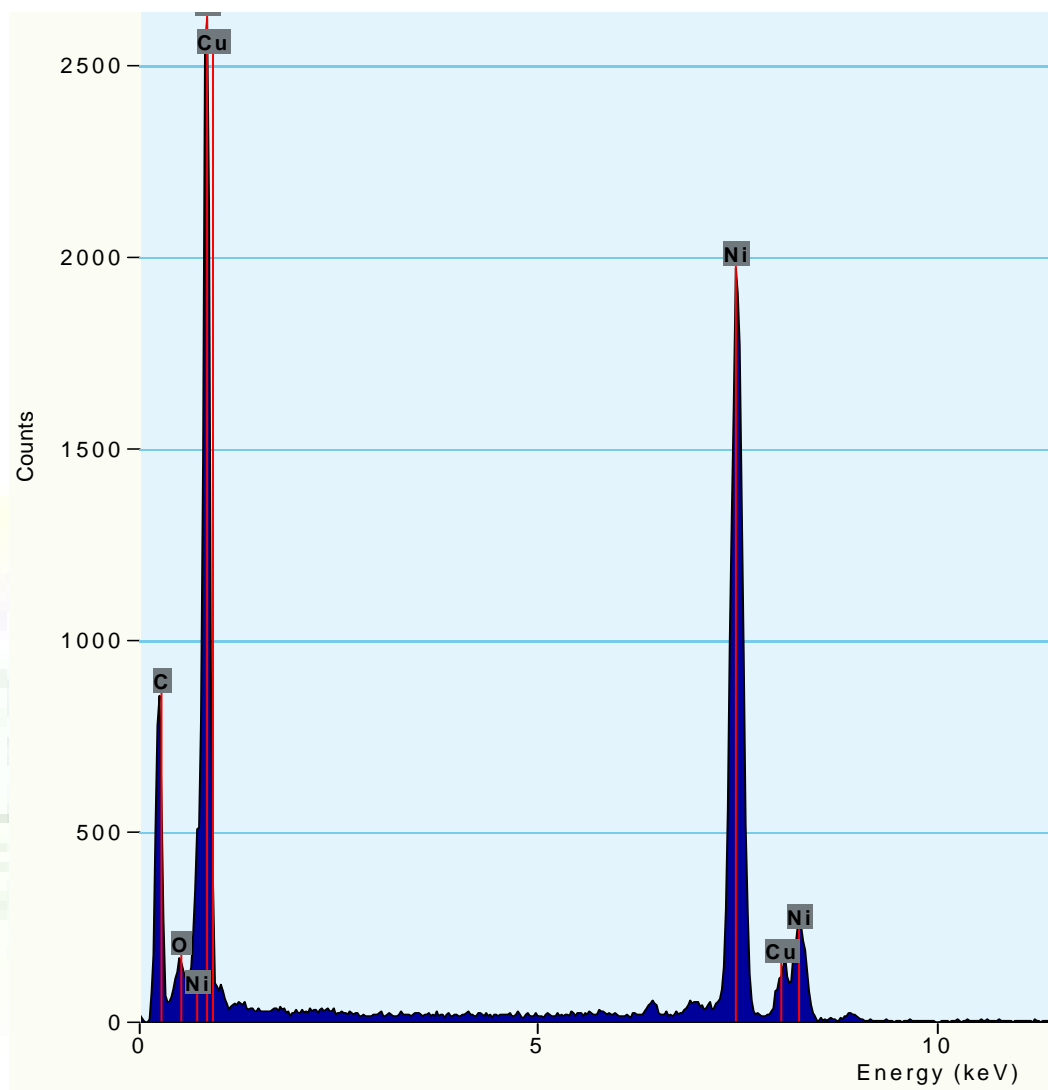


Fig. 4.22 EDX of the metal particle at tip of the carbon nanotubes.

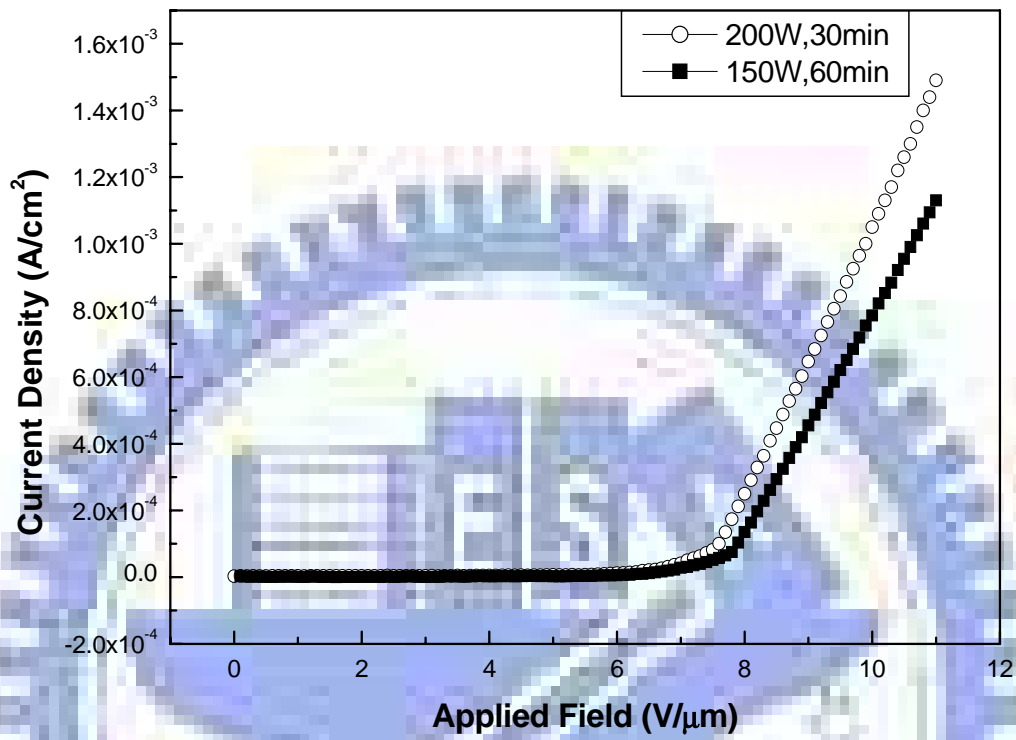


Fig. 4.23 Field emission properties of CNTs by sol-gel method on diode structure.